JOURNAL OF MECHANICS OF CONTINUA AND MATHEMATICAL SCIENCES
www.journalimcms.org

ISSN (Online) : 2454 -7190 Vol.-19, No.-11, November (2024) pp 126 - 143 ISSN (Print) 0973-8975

ROLE OF VACCINATION ON THE CO-INFECTION MODEL WITH COVID-19 ASSOCIATED WITH DIABETES

Md. Abdul Hye[1], Md. Haider Ali Biswas[2], Mohammed Forhad Uddin[3]

[1] Department of Mathematics and Statistics, Bangladesh University of Business and Technology (BUBT), Dhaka-1216, Bangladesh.

[2] Mathematics Discipline, Khulna University, Khulna-9208, Bangladesh.

[1, 3] Department of Mathematics, Bangladesh University of Engineering and Technology (BUET), Dhaka-1000, Bangladesh.

Email: [1]abdul@bubt.edu.bd, [2]mhabiswas@yahoo.com, [3] farhad@math.buet.ac.bd

Corresponding Author: **Md. Abdul Hye**

https://doi.org/10.26782/jmcms.2024.11.00009

(Received: August 01, 2024; Revised: September 20, 2024; Accepted: October 18, 2024)

Abstract

COVID-19 infection is particularly dangerous for individuals with comorbidities such as kidney disease and diabetes due to weakened immunity. While the pandemic has impacted people of all ages and socioeconomic backgrounds, those with underlying medical conditions are more susceptible to severe outcomes. However, the role of vaccination in the co-infection dynamics of COVID-19 among diabetic patients is not well-represented in the literature. This study examines the unique challenges presented by the co-infection of COVID-19 in individuals with diabetes, focusing on disease transmission dynamics. We employ a mathematical modeling approach using a seven-compartment model that incorporates vaccination and comorbidities like diabetes to analyze the dynamics of COVID-19 outbreaks. Analytical investigations were conducted to demonstrate the solutions' existence, boundedness, positivity, and sensitivity. After calculating the basic reproduction number, we performed a stability analysis of the model's equilibrium points. Our findings indicate that when the reproduction number is less than unity, the disease-free equilibrium is both locally and globally stable. Furthermore, as the vaccination rate increases, the incidence of COVID-19 and its co-infections with diabetes decreases. These results suggest that effective disease treatment strategies should consider the potential impact of vaccination on the co-infection of COVID-19 in diabetic patients.

Keywords: COVID-19, Diabetes, Comorbidity, Co-infection, Vaccination

I. Introduction

COVID-19, caused by the SARS-CoV-2 virus, emerged as a significant global health threat in late 2019 [XV]. Identified initially in Wuhan, Hubei province of China, the disease quickly spread globally, leading the World Health Organization (WHO) to declare it a pandemic in March 2020. The virus's origins have been the subject of

extensive research, with studies suggesting that it likely jumped from an animal host, potentially bats, to humans, possibly with an intermediate host involved [XXII]. The primary transmission mode is through respiratory droplets, although contact with contaminated surfaces can also result in infection [XII]. The disease manifests symptoms from mild cough and fever to severe respiratory distress, with older adults and those with underlying health conditions particularly vulnerable [XVII]. Efforts to combat its spread have included worldwide vaccination campaigns, the efficacy of which has been a primary focus of scientific research and public health initiatives [XVI]. While there hasn't been an approved vaccine or antiviral treatment for COVID-19, many countries and people have adopted non-pharmaceutical measures like wearing face masks in public, practicing social distancing, and enforcing lockdowns to help curb the spread of the virus. [XX, VIII]. Recent epidemiological research suggests that it's important to consider the co-existence of COVID-19 and comorbidities like diabetes, lung disease, and heart disease. Individuals with these underlying conditions appear to have a heightened risk of contracting the virus [II, XIX]. Bjorgul, Novicoff, and Saleh [IV] characterize comorbidities as diseases or medical conditions that coexist with the primary diagnosis under consideration while not sharing an origin or causal relationship. Diabetes mellitus is a chronic metabolic disorder characterized by high blood sugar levels over a prolonged period. It is a major public health concern worldwide, affecting millions of individuals and contributing significantly to morbidity and mortality. The disease is categorized mainly into Type 1 diabetes (T1D), Type 2 diabetes (T2D), and gestational diabetes. T1D is an autoimmune condition where the body's immune system attacks and destroys insulin-producing beta cells in the pancreas. This form of diabetes is less common, accounting for about 5-10% of all diabetes cases. T1D typically manifests in childhood or adolescence [I, VI].T2D is the most prevalent form of diabetes, accounting for about 90-95% of all cases. Models play a pivotal role in understanding the transmission dynamics of infectious diseases. The utilization of mathematical models for examining infectious diseases has seen a marked rise in recent periods, as indicated by studies [XIII, III]. Hence, the emergence of a branch has been done, which is called mathematical epidemiology. Frequent diagnostic tests, the availability of clinical data, and electronic surveillance have facilitated mathematical models' applications to critically examine scientific hypotheses and design real-life strategies for controlling diseases [XXI]. According to WHO, the COVID-19 vaccine is highly effective, but a small percentage of people will still get ill from COVID-19 after vaccination [V,XVII,IX].Everybody could also pass the virus on to others who are not vaccinated. Mathematical models provided invaluable insights into potential transmission dynamics, peak infection times, and the potential impact of interventions [XVIII]. These models also identified key parameters like the basic reproduction number (R_0) and offered scenarios based on various containment strategies. This study investigates the complexities of COVID-19 and diabetes co-infections and explores vaccination strategies aimed at mitigating disease severity and spread. Very recently Hye, M.A. et al. noted that limited research exists on COVID-19 co-infection with kidney disease, highlighting the need for mathematical models to understand their interaction [XXIII, XXIV]. Utilizing a compartmental epidemic model with imperfect vaccination, we conduct analytical analyses and numerical simulations to compare the dynamics of COVID-19 among individuals with and without diabetes mellitus. Our

findings underscore the crucial need for focused, comprehensive studies on these co-infections in the ongoing fight against the COVID-19 pandemic.

II. Mathematical Model

We delved into a seven-compartment model for a randomized human population. The entire group is split into seven distinct categories, namely susceptible population (S), COVID-19 infected(I_C), covid-19 vaccinated susceptible (V) diabetic sensitive individuals (S_d), Co infected Covid-19 and diabetics(I_{cd}), Recover from Covid-19 (R_c), Recover from Covid-19 but with people with diabetes (R_{cd}). We assumed that the recruitment increases the susceptible population at a rate Π. All populations in each compartment suffer from a natural death rate μ. The susceptible population (S) acquires COVID-19 at the rate $f = \frac{\alpha(I_c+\gamma I_{cd})}{N}$, where α indicates the COVID-19 contact rate, γ Parameter alteration for higher infectiousness of co-infected persons due to comorbidity. Diabetes is becoming more common among people at this epidemiological rate at ϕ . Diabetes development rate θ in vaccinated susceptible persons. Vaccinated susceptible (V) acquire COVID-19 at a decreased rate$(1-\sigma)f$, where σ is the COVID-19 vaccine efficacy. COVID-19 vaccination rate τ_v from the susceptible populations. Diabetic susceptible (S_d) acquire COVID-19 at the rate ωf , where ω accounts for diabetics' greater susceptibility rate. χ_1, χ_2 indicate recovery metrics for COVID-19 based on individual groupings (I_c) and Covid-19 co-infected (I_{cd}) respectively. Reinfection rates η_1, η_2 for Individuals recovered from COVID-19 are in compartments R_c and R_{cd} respectively.

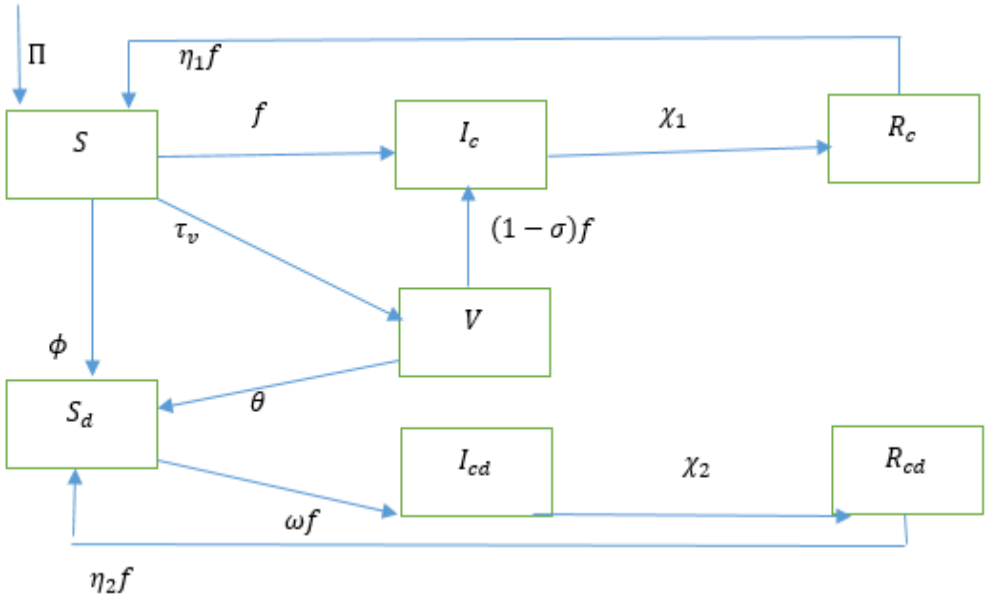

Fig. 1. The transmission dynamics of diabetes and COVID-19 co-infection are shown in a flow chart.

$$\frac{ds}{dt} = \Pi - fS - \tau_v S - \phi S - \mu S + +\eta_1 f R_c \quad (1)$$

$$\frac{ds_d}{dt} = \phi S + \theta V - \omega f S_d + +\eta_2 f R_{cd} - \mu S_d \quad (2)$$

$$\frac{dI_c}{dt} = fS + (1-\sigma)fV - \chi_1 I_c - \mu I_c \quad (3)$$

$$\frac{dI_{cd}}{dt} = \omega f S_d - \chi_2 I_{cd} - \mu I_{cd} \quad (4)$$

$$\frac{dV}{dt} = \tau_v S - \theta V - (1-\sigma)fV - \mu V \quad (5)$$

$$\frac{dR_c}{dt} = \chi_1 I_c - \eta_1 f R_c - \mu R_c \quad (6)$$

$$\frac{dR_{cd}}{dt} = \chi_2 I_{cd} - \eta_2 f R_{cd} - \mu R_{cd} \quad (7)$$

Table 1: Parameter description with values

Parameter	Biological Interpretation	Value	References
Π	Recruitment rate to susceptible populations	630	calculated
τ_v	Vaccination rate COVID-19 (rate of people who are vaccinated)	0.25	[IV]
α	COVID-19 contact rate	1.2	Fitted
γ	Parameter alteration for higher infectiousness of co-infected persons due to comorbidity	0.5776	Fitted
σ	COVID-19 vaccine efficacy	0.70	[XII]
η_1	The compartment R_c indicates the reinfection rates for individuals recovered from COVID-19	0.0013	Estimated
η_2	The compartment R_c indicates the reinfection rates for individuals recovered from COVID-19	0.0013	Estimated
ω	Accounts for diabetics' greater susceptibility rate.	0.60	[XV]
ϕ	Rate of Diabetes development for susceptible humans	0.0028	Estimated
θ	Diabetes increased rate θ in vaccinated susceptible persons	0.018	Fitted
χ_1	Recovery rates for COVID-19 within the I_c compartment.	0.00014	Fitted
χ_2	Recovery rates for COVID-19 within the I_{cd} compartment.	0.0124	Fitted
μ	Natural death rate	0.000038	calculated

Theorem 1. All the populations of the system with positive initial conditions are nonnegative let $S > 0, S_d > 0, V \geq 0, I_c \geq 0, I_{cd} \geq 0, R_c \geq 0, R_{cd} \geq 0$, then $(S, S_d, V, I_c, I_{cd}, R_c, R_{cd})$ of the system are positive for all time $t > 0$.

$$\frac{ds}{dt} = \Pi - fS - \tau_v S - \phi S - \mu S + \eta_1 f R_c$$

By using the technique of variable separation $\frac{dS}{dt}$ can be reduced to

$$\frac{dS}{dt} > -(f + \tau_v + \phi + \mu)S$$

$$\frac{dS}{S} > -(f + \tau_v + \phi + \mu)dt$$

Then, the above equation is integrated to yield the solution below

$$S(t) > S_0 e^{-\int_0^t (f+\tau_v+\phi+\mu)dt} > 0 \tag{8}$$

Since the initial value, $S(0)$, and the exponential functions in equation (8) are always positive

Hence, $S(t)$is positive. Using a similar technique to verify other equations of equations (1) to (7), this shows that

$$S > 0, S_d > 0, V \geq 0, I_c \geq 0, I_{cd} \geq 0, R_c \geq 0, R_{cd} \geq 0$$

Theorem 2. The dynamical system (1) to (7) is positively invariant in the closed invariant set $\mathrm{Z}_1 = \{(S, S_d, V, I_c, I_{cd}, R_c, R_{cd}) \epsilon \mathbb{R}_+^7 : N \leq \frac{\Pi}{\mu}\}$

To obtain an invariant region that shows that the solution is bounded, we have

$$N = S + S_d + V + I_c + I_{cd} + R_c + R_{cd}$$

$$\frac{dN}{dt} = \frac{dS}{dt} + \frac{dS_d}{dt} + \frac{dV}{dt} + \frac{dI_c}{dt} + \frac{dI_{cd}}{dt} + \frac{dR_c}{dt} + \frac{dR_{cd}}{dt}$$

$$\frac{dN}{dt} = \Pi - N\mu$$

The general solution of the equation $N(t) = \frac{\Pi}{\mu} + \left(N(0) - \frac{\Pi}{\mu}\right) e^{-\mu t}$, where

$$N(t) = N(0) \; at \; t = 0.$$

We can follow that $N(t) \to \frac{\Pi}{\mu}$ as $t \to \infty$. Thus, it can be concluded that $N(t)$ is bounded as $0 \leq N(t) \leq \frac{\Pi}{\mu}$.

Hence, the feasible region of the model in the nonnegative region is defined as

$$\mathrm{Z} = \{(S, S_d, V, I_c, I_{cd}, R_c, R_{cd}) \in \mathbb{R}_+^7 + : N \leq \frac{\Pi}{\mu}\} \tag{9}$$

III. Analytical Analysis of Co-infection Model

We compute the equilibrium and provide conditions for their existence. We also determine the reproduction number of the model and use it to study the stability of the computed equilibria and the sensitivity of the model.

III.i. The disease-free steady-state Equilibrium Points of the Model

The disease-free equilibrium of equations (1) to (7) is given by

$$I_c = 0,\ I_{cd} = 0, R_c = 0, R_{cd} = 0$$

$$\frac{dS}{dt} = \frac{dS_d}{dt} = \frac{dV}{dt} = \frac{dI_c}{dt} = \frac{dI_{cd}}{dt} = \frac{dR_c}{dt} = \frac{dR_{cd}}{dt} = 0$$

$$S = \frac{\Pi}{(\tau_v+\phi+\mu)}$$

$$S_d = \frac{\Pi\phi(\theta+\mu)(\tau_v+\phi+\mu)+\theta\tau_v\Pi}{\mu(\tau_v+\phi+\mu)^2(\theta+\mu)}$$

$$V = \frac{\tau_v\Pi}{(\theta+\mu)(\tau_v+\phi+\mu)}$$

Hence, the disease-free equilibrium point (DFEP) of the COVID-19 co-infection model is

$$\mathrm{E}_0 = \left(\frac{\Pi}{(\tau_v+\phi+\mu)}, \frac{\Pi\phi(\theta+\mu)(\tau_v+\phi+\mu)+\theta\tau_v\Pi}{\mu(\tau_v+\phi+\mu)^2(\theta+\mu)}, \frac{\tau_v\Pi}{(\theta+\mu)(\tau_v+\phi+\mu)}, 0,0,0,0\right) \quad (10)$$

III.ii. The basic reproduction number R_0

$$F = \begin{pmatrix} \frac{\alpha S+(1-\sigma)\alpha V}{N} & \frac{\alpha\gamma S+(1-\sigma)\gamma\alpha V}{N} \\ \frac{\omega\alpha S_d}{N} & \frac{\omega\alpha\gamma S_d}{N} \end{pmatrix},\ V = \begin{pmatrix} (\chi_1+\mu) & 0 \\ 0 & (\chi_2+\mu) \end{pmatrix}$$

$$FV^{-1} = \begin{pmatrix} \frac{\alpha S+(1-\sigma)\alpha V}{N} & \frac{\alpha\gamma S+(1-\sigma)\gamma\alpha V}{N} \\ \frac{\omega\alpha S_d}{N} & \frac{\omega\alpha\gamma S_d}{N} \end{pmatrix} \begin{pmatrix} \frac{1}{(\chi_1+\mu)} & 0 \\ 0 & \frac{1}{(\chi_2+\mu)} \end{pmatrix}$$

$$= \begin{pmatrix} \frac{\alpha S+(1-\sigma)\alpha V}{N(\chi_1+\mu)} & \frac{\alpha\gamma S+(1-\sigma)\gamma\alpha V}{N(\chi_2+\mu)} \\ \frac{\omega\alpha S_d}{N(\chi_1+\mu)} & \frac{\omega\alpha\gamma S_d}{N(\chi_2+\mu)} \end{pmatrix}$$

$$FV^{-1} - \lambda I = \begin{pmatrix} \frac{\alpha S+(1-\sigma)\alpha V}{N(\chi_1+\mu)} - \lambda & \frac{\alpha\gamma S+(1-\sigma)\gamma\alpha V}{N(\chi_2+\mu)} \\ \frac{\omega\alpha S_d}{N(\chi_1+\mu)} & \frac{\omega\alpha\gamma S_d}{N(\chi_2+\mu)} - \lambda \end{pmatrix}$$

The largest eigenvalue is the basic reproduction number.

$$R_0 = Max\left(\frac{\alpha\Pi(\theta+\mu+\tau_v-\sigma\tau_v)}{N(\chi_1+\mu)(\theta+\mu)(\tau_v-\sigma\tau_v)}, \frac{\Pi\phi(\theta+\mu)(\tau_v+\phi+\mu)+\theta\tau_v\Pi}{\mu(\tau_v+\phi+\mu)^2(\theta+\mu)}\right) \quad (11)$$

III.iii. Existence of Endemic equilibrium points

For the equilibrium points of the equations (1) to (7),

$$\frac{dS}{dt} = \frac{dS_d}{dt} = \frac{dV}{dt} = \frac{dI_c}{dt} = \frac{dI_{cd}}{dt} = \frac{dR_c}{dt} = \frac{dR_{cd}}{dt} = 0 \quad (12)$$

Let, $E^* = (S^*, S_d^*, V^*, I_c^*, I_{cd}^*, R_c^*, R_{cd}^*)$ represents the disease equilibrium point. The components of E^* are the positive solutions of the nonlinear system of equations

$$S^* == \frac{\Pi}{(f^*+k_1)}$$

$$S_d^* = \frac{\frac{\phi\Pi}{(f^*+k_1)}+\frac{\theta\Pi\tau_v}{(\theta+(1-\sigma)f^*+\mu)(f^*+k_1)}}{(\omega f^*+\mu)}$$

$$I_c^* = \frac{\frac{\alpha(I_C^*+\gamma I_{cd}^*)}{N}S^*+(1-\sigma)\frac{\alpha(I_C^*+\gamma I_{cd}^*)}{N}V^*+\eta_1\frac{\alpha(I_C^*+\gamma I_{cd}^*)}{N}R_c^*}{(\chi_1+\mu)}$$

$$= \frac{f^*S^*+(1-\sigma)f^*V^*+\eta_1 f^*R_c^*}{(\chi_1+\mu)}$$

$$I_c^* = \frac{(\mu+\eta_1 f^*)}{(k_3(\mu+\eta_1 f^*)-\eta_1 f^*\chi_1)}\left(\frac{f^*\Pi}{(f^*+k_1)}+\frac{(1-\sigma)f^*\tau_v\Pi}{(\theta+(1-\sigma)f^*+\mu)(f^*+k_1)}\right)$$

$$I_{cd}^* = \frac{(\eta_2 f^*+\mu)}{(\omega f^*+\mu)(k_2(\eta_2 f^*+\mu)-\eta_2 f^*\chi_2)}\left(\frac{\omega f^*\phi\Pi}{(f^*+k_1)}+\frac{\theta\Pi\tau_v}{(\theta+(1-\sigma)f^*+\mu)(f^*+k_1)}\right)$$

$$V^* = \frac{\tau_v\Pi}{(\theta+(1-\sigma)f^*+\mu)(f^*+k_1)}$$

$$R_c^* = \frac{\chi_1 I_c^*}{(\mu+\eta_1 f^*)}$$

$$R_{cd}^* = \frac{\chi_2 I_{cd}^*}{(\eta_2 f^*+\mu)} \tag{13}$$

Where, $k_1 = \tau+\phi+\mu, k_2 = (\chi_2+\mu), k_3 = (\chi_1+\mu)$

Substituting the above expressions into the force of infection, at a steady state, gives the following polynomial

$$D_1(f^*)^5 + D_2(f^*)^4 + D_3(f^*)^3 + D_4(f^*)^2 + D_5 f^* + D_6 = 0 \tag{14}$$

Where, $D_1 = \eta_2 k_2\omega\ \phi\Pi\eta_2\gamma\theta\eta_1\chi_1 + (1-\sigma)\omega k_2\eta_2 - \eta_2\chi_2(1-\sigma)\omega$

$$\begin{aligned} D_2 = {} & \theta\omega k_2\eta_2 + \mu\omega k_2\eta_2 + k_2\eta_2 k_1(1-\sigma)\omega + k_2\eta_2\mu(1-\sigma) + k_2\mu(1-\sigma)\omega \\ & - \theta\omega\eta_2\chi_2 - \eta_2\chi_2\mu\omega - \eta_2\chi_2 k_1(1-\sigma)\omega - \eta_2\chi_2\mu(1-\sigma) \\ & - \alpha\mu\Pi\omega(1-\sigma)\eta_2\chi_2 - \omega\eta_2 k_2\eta_1\alpha(1-\sigma)\tau_v\Pi \\ & + \eta_2\chi_2\omega\eta_1\alpha(1-\sigma)\tau_v\Pi - \omega\phi\Pi\eta_2\gamma k_3\eta_1(1-\sigma) \\ & + \omega\ \phi\Pi\eta_2\gamma\eta_1\chi_1(1-\sigma) \end{aligned}$$

$$\begin{aligned} D_3 = {} & k_1\theta\omega k_2\eta_2 + k_2\eta_2 k_1\mu\omega + k_2\eta_2\mu\theta + k_2\eta_2\mu^2 + k_2\eta_2\mu k_1(1-\sigma) + \theta\omega k_2\mu \\ & + k_2\mu^2\omega + k_2\mu k_1(1-\sigma)\omega + k_2\mu^2(1-\sigma) - \eta_2\chi_2 k_1\theta\omega \\ & - \eta_2\chi_2 k_1\mu\omega - \eta_2\chi_2\mu\theta - \eta_2\chi_2\mu^2 - \eta_2\chi_2\mu k_1(1-\sigma) \\ & - \gamma\mu\omega\phi\Pi k_3\eta_1(1-\sigma) + \gamma\mu\omega\phi\Pi\eta_1\chi_1(1-\sigma) + \omega\ \phi\Pi\eta_2\gamma\mu\eta_1\chi_1 \\ & - \omega\ \phi\Pi\eta_2\gamma\theta k_3\eta_1 + \omega\ \phi\Pi\eta_2\gamma\theta\eta_1\chi_1 - \omega\ \phi\Pi\eta_2\gamma k_3\mu(1-\sigma) \\ & + \eta_1\alpha(1-\sigma)\tau_v\Pi\eta_2\chi_2\mu - \eta_2 k_2\mu\eta_1\alpha(1-\sigma)\tau_v\Pi \\ & - k_2\mu\omega\eta_1\alpha(1-\sigma)\tau_v\Pi + \eta_2\chi_2\omega\alpha(1-\sigma)\tau_v\Pi\mu \\ & - \eta_2 k_2\mu^2\alpha(1-\sigma)\tau_v\Pi - \omega\eta_2 k_2\alpha(1-\sigma)\tau_v\Pi\mu \\ & + \alpha\Pi\eta_2\chi_2\mu^2(1-\sigma) + \alpha\mu^2\Pi\omega\eta_2\chi_2 - \omega(1-\sigma)k_2\mu^2\alpha\Pi \\ & + \omega\theta k_2\eta_2\alpha\mu\Pi - \omega(1-\sigma)k_2\eta_2\alpha\mu\Pi - k_2\eta_2\omega\mu^2\alpha\Pi \\ & - k_2\eta_2\mu^2(1-\sigma)\alpha\Pi \end{aligned}$$

$$D_4 = k_2\eta_2\mu^2k_1 + k_2\mu k_1\theta\omega + k_2\mu^2k_1\omega + k_2\mu^2\theta + k_2\mu^2\mu + k_2\mu^2k_1(1-\sigma) - \eta_2\chi_2\mu k_1\theta - \eta_2\chi_2\mu k_1\mu - k_2\eta_2\theta\mu^2\alpha\Pi - k_2\eta_2\mu^2\alpha\mu\Pi - \omega\theta k_2\mu^2\alpha\Pi - \omega\mu^3k_2\alpha\Pi - \alpha\Pi k_2\mu^3\ (1-\sigma) + \alpha\mu^2\Pi\theta\eta_2\chi_2 + \alpha\Pi\,\mu^3\eta_2\chi_2 - k_2\mu^2\omega\alpha(1-\sigma)\tau_v\Pi + \eta_2\chi_2\mu^2\alpha(1-\sigma)\tau_v\Pi - k_2\mu\eta_1\alpha(1-\sigma)\tau_v\Pi - k_3\mu\theta\omega\ \phi\Pi\eta_2\gamma - \omega\ \phi\Pi\eta_2\gamma k_3\mu^2 - \gamma\mu\omega\phi\Pi\theta k_3\eta_1 + \gamma\mu\omega\phi\Pi\theta\eta_1\chi_1 - \gamma\mu\omega\phi\Pi k_3\mu(1-\sigma) - \gamma\mu\omega\phi\Pi\mu k_3\eta_1 + \gamma\mu\omega\phi\Pi\mu\eta_1\chi_1 - k_3\eta_1\eta_2\gamma\theta\Pi\tau_v + \eta_1\chi_1\eta_2\gamma\theta\Pi\tau_v$$

$$D_5 = k_2\mu^2k_1\theta + k_2\mu^2k_1 + \mu k_1\theta - k_3\eta_1\theta\Pi\tau_v\gamma\mu + \eta_1\chi_1\theta\Pi\tau_v\gamma\mu - k_3\mu\eta_2\gamma\theta\Pi\tau_v - \gamma\mu\omega\phi\Pi k_3\mu^2 - k_3\mu\theta\gamma\mu\omega\phi\Pi - \mu k_3\eta_1 - \alpha\Pi k_2\mu^4 - \theta k_2\mu^3\alpha\Pi$$

$$D_6 = \alpha\Pi\,\mu^3\eta_2\chi_2 + k_3k_2(1-\sigma)\mu^2\theta\Pi\tau_v\gamma(1-R_0) \quad (15)$$

The components of the EEP are determined by solving for f^* from the polynomial in equation (14) and substituting the positive solutions into the expressions in equation (12). Additionally, from equation (15), it is clear that the coefficient D_1 is always positive. Meanwhile, D_6 is positive if R_0 is less than one and negative if R_0 is greater than one. The following conclusions can be drawn:

The system of (1) has (i) four or two endemic equilibriums if $D_3 > 0, D_4 < 0, Q_4 > 0$ and $R_0 < 1$

(ii) two endemic equilibrium if $D_3 > 0 D_4 > 0, D_5 < 0$ and $R_0 < 1$

(iii) no endemic equilibrium otherwise, if $R_0 < 1$.

III.iv. Global Stability of DFE and the EE point

$$T = S - S^* - S^*\ln\left(\frac{S}{S^*}\right) + \frac{1}{2}I_c^2$$

$$\frac{dT}{dt} = \left(1 - \frac{S^*}{S}\right)\frac{dS}{dt} + I_c\frac{dI_c}{dt}$$

$$= \left(1 - \frac{S^*}{S}\right)[\Pi - (f+\theta+\mu)S] + I_c[fS - P_1I_c]$$

$$= \left(1 - \frac{S^*}{S}\right)[\Pi - (f+\theta+\mu)S] + I_c^2[\frac{\alpha S}{N} - P_1]$$

At the COVID-19 free equilibrium point (CFE) we have the following form

$$\frac{dT}{dt} = -\frac{(f+\theta+\mu)(S-S^*)^2}{S} + I_c^2(\frac{\alpha S}{N} - P_1)$$

$$\leq -\frac{(f+\theta+\mu)(S-S^*)^2}{S} + \frac{I_c^2}{P_1}(R_{0c} - 1)$$

Hence, $T < 0$ if and only if $R_{0c} \leq 1$. Therefore, L is a Lyapunov function for the system (1) to (7). It follows by La Salle's Invariance Principle [XIII], that the CFE of the model (1) to (7) are globally stable.
The Lyapunov function is defined as

$$L = \frac{1}{2}[(S - S^*) + (S_d - S_d^*) + (V - V^*) + (I_c - I_c^*) + (I_{cd} - I_{cd}^*) + (R_c - R_c^*) + (R_{cd} - R_{cd}^*)]^2$$

The function L needs to be proven to determine whether the Lyapunov function is valid or invalid for Ψ^*

$$L(\Psi^*) = L(S^*, S_d^*, V^*, I_c^*, I_{cd}^*, R_c^*, R_{cd}^*)$$

$$L(\Psi^*) = \frac{1}{2}[(S - S^*) + (S_d - S_d^*) + (V - V^*) + (I_c - I_c^*) + (I_{cd} - I_{cd}^*) + (R_c - R_c^*) + (R_{cd} - R_{cd}^*)]^2$$

It is proven that $L(\Psi^*) = 0$

$$L(\Psi) = \frac{1}{2}[(S - S^*) + (S_d - S_d^*) + (V - V^*) + (I_c - I_c^*) + (I_{cd} - I_{cd}^*) + (R_c - R_c^*) + (R_{cd} - R_{cd}^*)]^2$$

Because $\forall\ (S, S_d, V, I_c, I_{cd}, R_c, R_{cd}) \neq (, S_d^0, V^0, I_c^0, I_{cd}^0, R_c^0, R_{cd}^0)$, so that it is shown that $L(\Psi) > 0$.

$$\frac{dL}{dt} = [(S - S^*) + (S_d - S_d^*) + (V - V^*) + (I_c - I_c^*) + (I_{cd} - I_{cd}^*) + (R_c - R_c^*) + (R_{cd} - R_{cd}^*)] + \frac{d}{dt}[S + S_d + V + I_c + I_{cd} + R_c + R_{cd}]$$

$$= [(S - S^*) + (S_d - S_d^*) + (V - V^*) + (I_c - I_c^*) + (I_{cd} - I_{cd}^*) + (R_c - R_c^*) + (R_{cd} - R_{cd}^*)][\Pi - \mu(S + S_d + V + I_c + I_{cd} + R_c + R_{cd})]$$

Let

$$\Pi = \mu(S^* + S_d^* + V^* + I_c^* + I_{cd}^* + R_c^* + R_{cd}^*)]$$

Now,$= [(S - S^*) + (S_d - S_d^*) + (V - V^*) + (I_c - I_c^*) + (I_{cd} - I_{cd}^*) + (R_c - R_c^*) + (R_{cd} - R_{cd}^*)] \times [-\mu((S - S^*) + (S_d - S_d^*) + (V - V^*) + (I_c - I_c^*) + (I_{cd} - I_{cd}^*) + (R_c - R_c^*) + (R_{cd} - R_{cd}^*)]$

$$= -[(S - S^*) + (S_d - S_d^*) + (V - V^*) + (I_c - I_c^*) + (I_{cd} - I_{cd}^*) + (R_c - R_c^*) + (R_{cd} - R_{cd}^*)] \times [\mu((S - S^*) + (S_d - S_d^*) + (V - V^*) + (I_c - I_c^*) + (I_{cd} - I_{cd}^*) + (R_c - R_c^*) + (R_{cd} - R_{cd}^*)]$$

Based on the description above, it can be concluded that $\frac{dL}{dt} < 0$ if $R_0 > 1$ and $\frac{dL}{dt} = 0$ if $S = S^*, S_d = S_d^*, V = V^*, I_c = I_c^*, I_{cd} = I_{cd}^*, R_c = R_c^*, R_{cd} = R_{cd}^*$. Hence, by LaSalle's invariance principle, it means that the endemic equilibrium point in the spread of COVID-19 is globally asymptotically stable if $R_0 > 1$.

III.v. Sensitivity Analysis

The sensitivity index quantifies the relative variation in a state variable in response to a parameter modification and is determined using sensitivity analysis. Using the method developed by Mousquer et al. [XI], we calculate the sensitivity indices of R_0 to the model parameters.

$$\beta_l^{R_0} = \frac{\partial R_0}{\partial l} \times \frac{l}{R_0}$$

$$\beta_\alpha^{R_0} = \frac{S+(1-\sigma)V}{N(\chi_1+\mu)} * \frac{1}{\frac{S+(1-\sigma)V}{N(\chi_1+\mu)}} = +1$$

$$\beta_\sigma^{R_0} = -\frac{\sigma\tau_v}{\theta+\mu+\tau_v-\sigma\tau_v}$$

$$\beta_{\tau_v}^{R_0} = \frac{-\tau_v\sigma(\theta+\mu)}{(\tau_v+\phi+\mu)(\theta+\mu-\tau_v-\sigma\tau_v)}$$

$$\beta_{\theta}^{R_0} == \frac{-\theta(\tau_v-\sigma\tau_v)}{(\theta+\mu)(\theta+\mu+\tau_v-\sigma\tau_v)}$$

$$\beta_{\chi_1}^{R_0} = -\frac{\chi_1}{(\chi_1+\mu)}$$

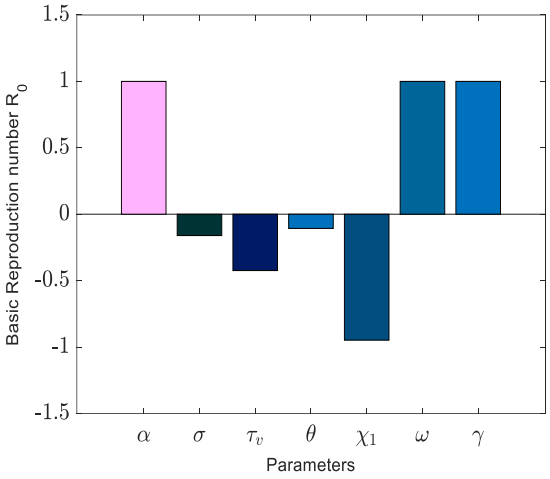

Table 2: Sensitivity indices of R_0

Parameter	Sensitivity index
α	+1.0000
σ	−0.1605
τ_v	−0.4240
θ	−0.1068
χ_1	−0.9482
ω	+1.0000
γ	+1.0000

Fig. 2: Effects of parameter variation on R_0.

Sensitivity analysis was conducted using the partial rank correlation coefficients (PRCCs) combined with the Latin hypercube sampling to assess the influence of each model parameter on the initial spread of the disease, represented by R_0 . Figure 2 illustrates the PRCCs, highlighting the ramifications of altering input parameters on the basic reproduction number,R_0. Parameters that have positive PRCCs enhance the initial transmission rates, whereas those with negative PRCCs curtail R_0. a closer look at Figure 2 helps pinpoint the most impactful parameters. Table 2's sensitivity indices reveal that when the values of α, ω, and γ surge, and other parameters remain constant, there's an uptick in R_0, suggesting increased disease endemicity due to the positive indices. Conversely, when the parameters $\sigma, \tau_v, \theta,$ and χ_1 drop and other values remain unchanged, R_0 diminishes, indicating a decline in disease endemicity given the negative indices. The contact rate α and the higher infectiousness of the co-infected person's rate γ are the most sensitive parameters.

IV. Parameter Estimation

The population of Bangladesh, as cited in source [XV], is approximately 170000000. Considering the first infected in Bangladesh, we try to explore the dynamics of worldwide daily and cumulative cases from April 2020. The data is retrieved from the World Health Organization (WHO)'s website [XV]: $S(0)$ = 0.93 * 170000000: This represents the initial number of susceptible individuals without comorbidities, calculated as 93% of the total population.$S_d(0)$ = 0.07 * 1700000: This denotes the initial number of susceptible individuals with comorbidities at 7% of the

total population.$I_c(0)$ = 412320: This indicates the initial number of COVID-19 cases without comorbidities. $I_{cd}(0)$ = 0: This is the initial number of recovered individuals from COVID-19 without comorbidities. $R_c = 0$: This signifies the initial number of COVID-19 cases with comorbidities. $R_{cd}(0)$ = 0: This represents the initial number of recovered individuals from COVID-19 with comorbidities. In our analysis, two optimization algorithms were utilized for data fitting purposes. The objective function is root mean error square $= \sqrt{\sum_{data\ i}^{n}(\boldsymbol{I_{C\ actual}(t_i) - I_{C\ model}(t_i)})^2}$ .The first was the genetic algorithm (GA), and the second was the fmincon algorithm, as documented in references [XIV].

This led to the calculation of the natural mortality rate per month as the inverse of life expectancy, resulting in a value of $\mu = \frac{1}{72.72\times365} = 0.000038$. Furthermore, the recruitment rate was approximated by manipulating the ratio of $\frac{\nabla}{\mu}$ to yield the initial population, resulting in $\nabla = 630$ individuals per day. Due to limited data on co-infections, we estimated certain co-infection-related parameters, while others were deduced from actual data. During the estimation process, the initial conditions of the state variables were set as delineated in Table 1.

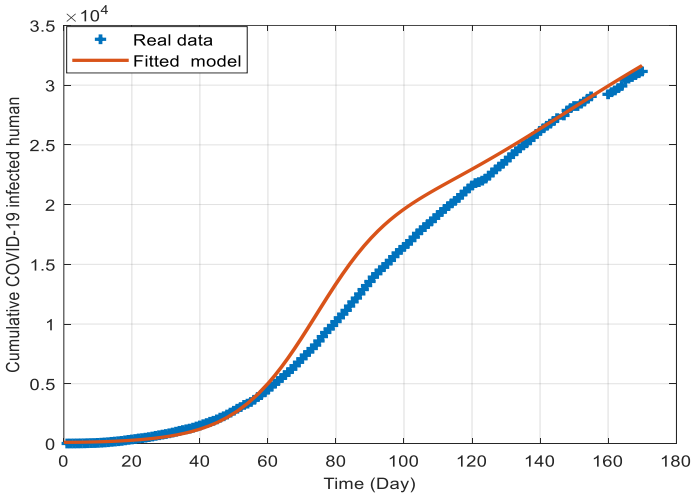

Fig. 4. Fitting the cumulative number of confirmed cases of COVID-19

Figure 4 demonstrates a strong fit between our model's projections (red line) and the actual cumulative COVID-19 infection data in Bangladesh from April 3rd to September 30th (blue line), indicating that the model effectively captures the real-world scenario.

V. Numerical Result and Discussions

We visualized the model's analytical outcomes through numerical simulations using MATLAB's ODE113 solver and parameter values from existing literature. Simulations under vaccination treatments examined how key factors affect COVID-19 transmission among diabetics and non-diabetics. When the effective reproduction number $R_0 < 1$, the post-vaccination model reaches a locally asymptotically stable

disease-free equilibrium, suggesting COVID-19 can be eradicated if initial conditions approach this point. The findings indicate that immunization primarily enhances the COVID-19 recovery rate.

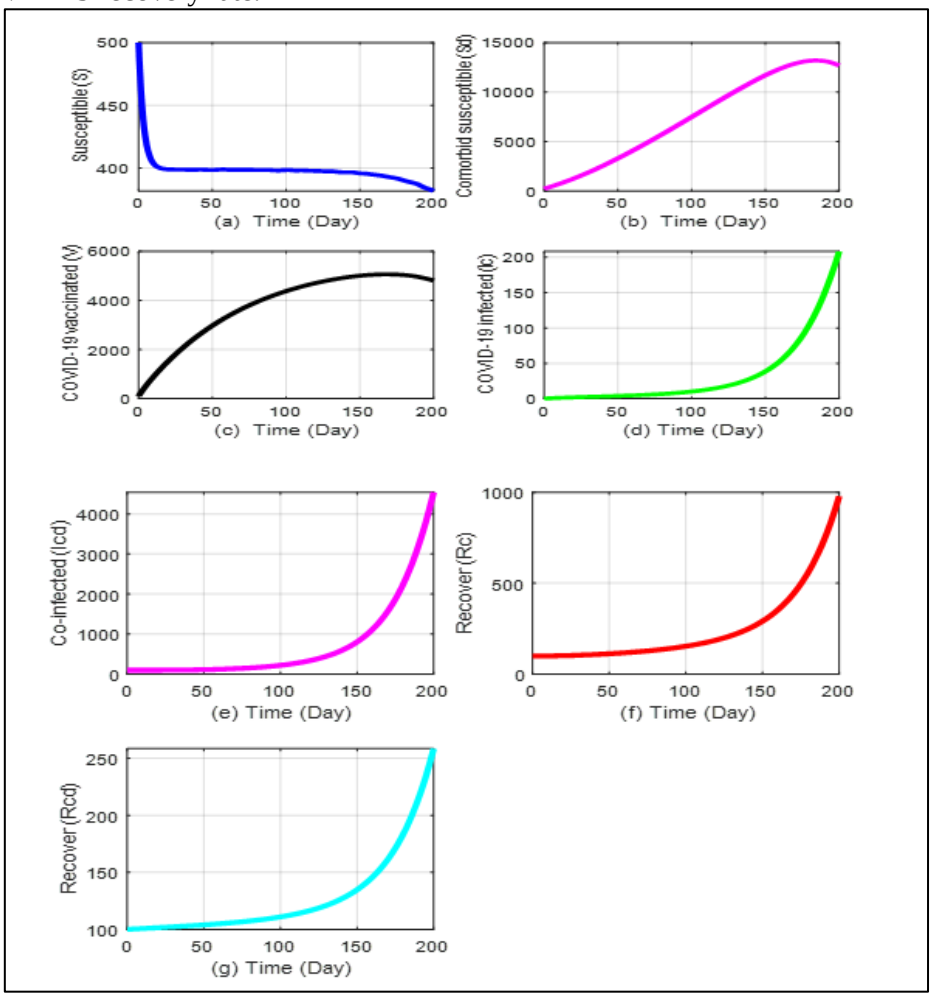

Fig. 5. Simulated population dynamics over 200 days with basic reproduction number $R_0 > 1$.

In Figure 5 simulations over 200 days with a basic reproduction number greater than 1 show declining susceptible populations, increasing infected and co-infected individuals, and vaccination rates surpassing recovery rates. Without vaccination or appropriate treatment, infections continue to rise but can be managed through physical distancing, increased vaccination, and self-immunity measures.

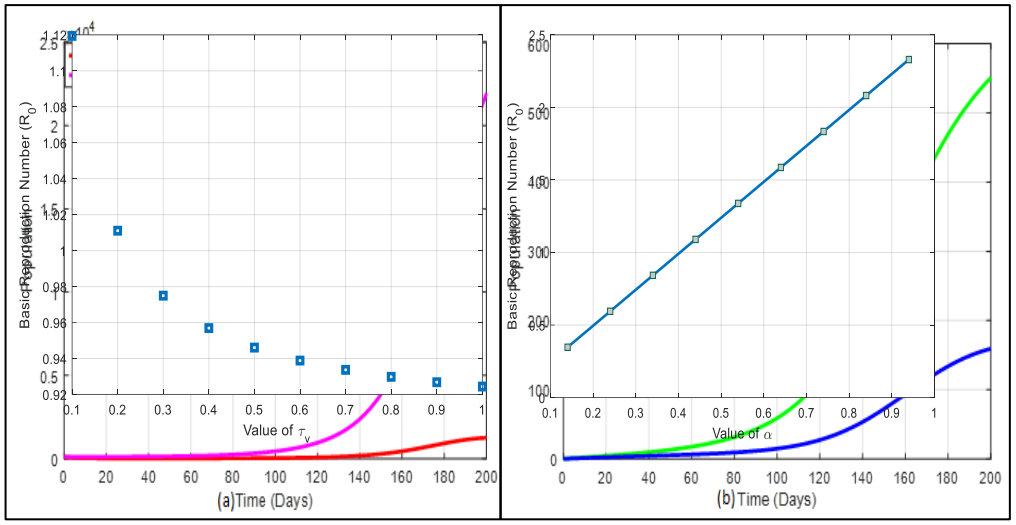

Fig. 6. Comparison of COVID-19 only and co-infection with diabetes: (a) Infected individuals; (b) Recovered individuals.

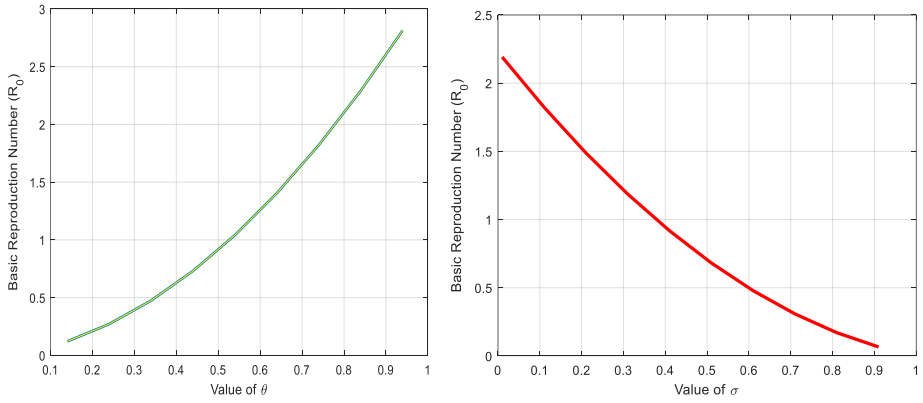

Fig. 7. (a) Increase in R_0 with diabetes rate θ among vaccinated susceptibles; (b) Decline in R_0 with COVID-19 vaccine efficacy rate σ.

Fig. 6 illustrates simulation outcomes without a vaccination strategy. In Fig. 6(a), the number of inpatients co-infected with COVID-19 and diabetes increases more rapidly than those infected with COVID-19 only. Fig. 6(b) shows that individuals infected with COVID-19 only recover more swiftly than those co-infected with diabetes. Figure 7(a) shows that increasing the diabetes rate (θ) among vaccinated susceptibles exponentially raises the basic reproduction number (R_0), indicating continued disease presence. Figs. 7(b) and 8(a) demonstrate that higher vaccine efficacy (σ) and increased vaccination rate (τ_v) significantly reduce R_0. Fig. 8(b) illustrates that R_0 increases linearly with the COVID-19 contact rate (α).

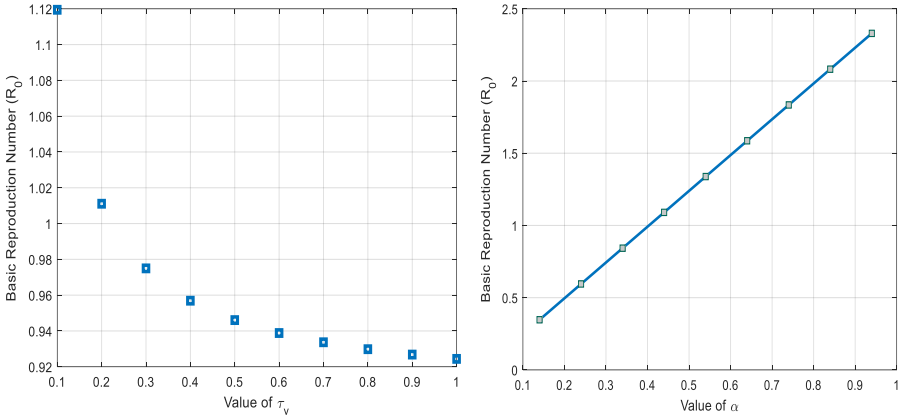

Fig. 8. (a) Decline in R_0 with increasing COVID-19 vaccination rate τ_v ; (b) Basic reproduction number R_0 in relation to COVID-19 contact rate α.

V.i. The Influence of Vaccination

Fig. 9(a) shows that without vaccination ($\tau_v = 0$), COVID-19 cases continue to rise. As the vaccination rate increases, there is a gradual decline in infections. Notably, at a moderate vaccination rate ($\tau_v = 0.10$), infections among diabetic individuals still increase slightly. However, a higher vaccination rate ($\tau_v = 0.20$)leads to a significant reduction in cases, as illustrated in Fig. 9(b).

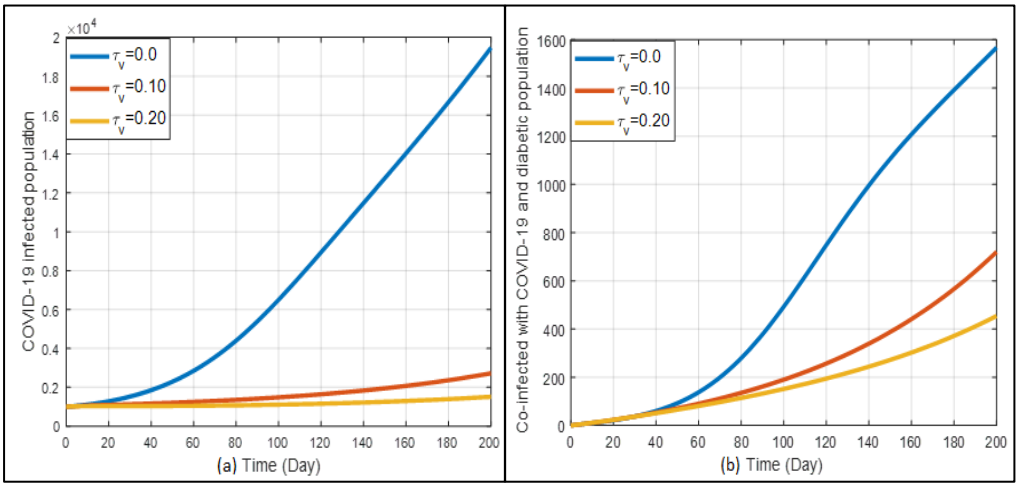

Fig. 9: (a) Simulations of infected case and (b) Co-infected case for different vaccination rate τ_v.

Fig. 10(a) demonstrates that increasing vaccine efficacy (σ) results in a marked decrease in COVID-19 infection cases, particularly at $\sigma = 0.70$. Similarly, Fig.10(b) indicates that higher vaccine efficacy reduces the number of co-infected cases of COVID-19 and diabetes over time. These findings underscore the crucial role of effective vaccination campaigns and high-efficacy vaccines in controlling the pandemic and protecting vulnerable populations.

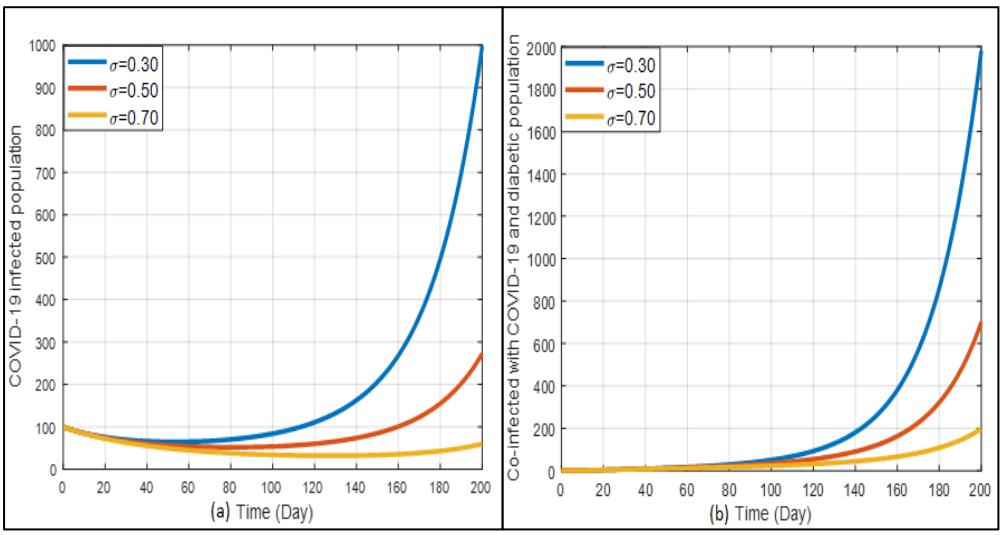

Fig. 10. (a) Simulations of infected cases effect of COVID-19 and (b) Co-infected cases of COVID-19 for various vaccine efficacy σ.

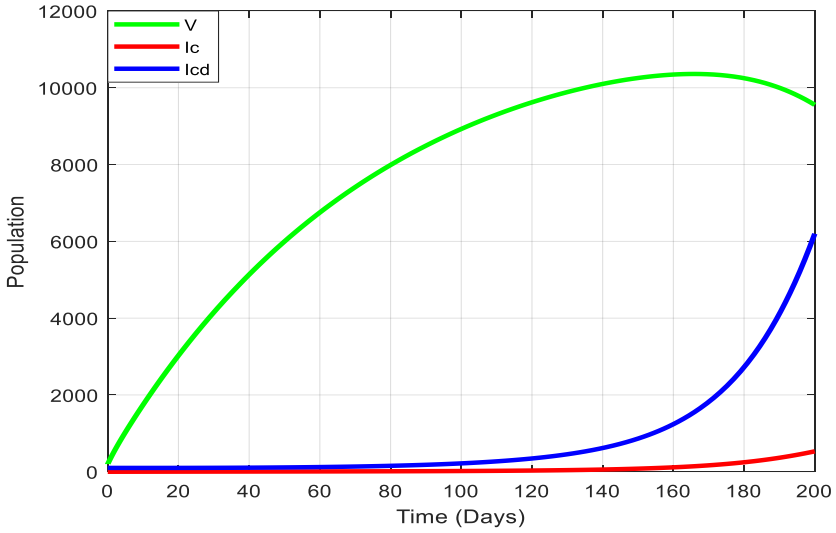

Fig. 11. Simulations of incidence case effect of vaccination

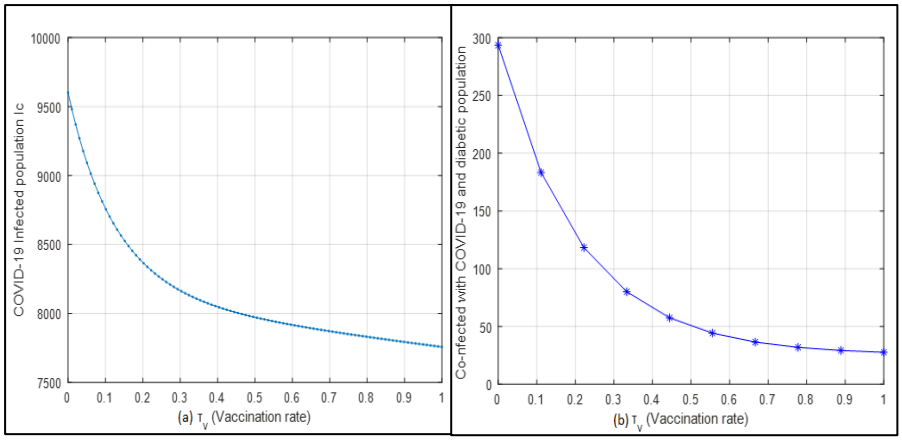

Fig. 12. (a) Role of vaccination on COVID-19 infected population(I_C); (b) Role of vaccination on COVID-19 co-infected population (I_{Cd})

Fig. 11 illustrates that as vaccination rates increase, COVID-19 infections and co-infections with diabetes decrease; conversely, decreasing vaccination rates lead to higher infection numbers. Fig. 12 confirms that higher vaccination rates significantly reduce both COVID-19 cases and co-infections with diabetes, underscoring the crucial role of vaccination in disease control.

VI. Conclusions

In conclusion, we developed a mathematical model to assess the impact of vaccination on individuals co-infected with COVID-19 and diabetes. The study emphasizes the significant threat COVID-19 poses to public health and highlights the vital role of vaccination in controlling disease spread. Our findings reveal that higher transmission rates can lead to persistent outbreaks, even with substantial vaccination coverage, particularly if vaccine efficacy is low. Vaccination was shown to reduce the incidence of COVID-19 and its co-infections with diabetes, demonstrating an inverse relationship between vaccination rates and disease spread. Although co-infections were present, the severity of the interaction between COVID-19 and diabetes did not intensify. Sensitivity analysis confirmed the importance of transmission rates in disease progression. These results underscore the need for widespread vaccination, especially among diabetic patients, and show how simulation models can assist in managing the complexities of co-infection. Future studies should investigate the effectiveness of different vaccine doses across diverse populations.

VII. Acknowledgment

We would like to express our endless gratitude to Bangladesh University of Engineering and Technology (BUET) primary research fund for its continuous logistic and financial support and valuable insights during this research.

Conflicts of Interest

The authors declare that there are no conflicts of interest regarding the publication of this manuscript.

References

I. Atkinson, M.A., G.S. Eisenbarth, and A.W. Michels, Type 1 diabetes. *The Lancet*, 383(9911), 69-82 (2014).

II. Azeez, A., J. Ndege, R. Mutambayi, Y. Qin, A mathematical model for TB/HIV co-infection treatment and transmission mechanism. *Asian Journal of Mathematics and Computer Research*, 22, 180-192 (2017)

III. Bai, Y., L. Yao, T. Wei, F. Tian, D.-Y. Jin, L. Chen, M. Wang, Presumed asymptomatic carrier transmission of COVID-19. *JAMA*, 323(14), 1406-1407 (2020).

IV. Bjorgul, K., W.M. Novicoff, K.J. Saleh, Evaluating comorbidities in total hip and knee arthroplasty: available instruments. *Journal of Orthopaedics and Traumatology*, 11, 203-209 (2010).

V. Dang, H.-A.H., M.N. Do, COVID-19 pandemic and the health and well-being of vulnerable people in Vietnam. *GLO Discussion Paper* (2022).

VI. DiMeglio, L.A., C. Evans-Molina, R.A. Oram, Type 1 diabetes. *The Lancet*, 391(10138), 2449-2462 (2018).

VII. Egonmwan, A., D. Okuonghae, Mathematical analysis of a tuberculosis model with imperfect vaccine. *International Journal of Biomathematics*, 12, 1950073 (2019).

VIII. Gomes, C.M., L.A. Favorito, J.V.T. Henriques, A.F. Canalini, K.M. Anzolch, R.d.C. Fernandes, C.H. Bellucci, C.S. Silva, M.L. Wroclawski, A.C.L. Pompeo, Impact of COVID-19 on clinical practice, income, health and lifestyle behavior of Brazilian urologists. *International Braz J Urol*, 46, 1042-1071 (2020).

IX. Iboi, E.A., C.N. Ngonghala, A.B. Gumel, Will an imperfect vaccine curtail the COVID-19 pandemic in the US? *Infectious Disease Modelling*, 5, 510-524 (2020).

X. Irena, T.K., S. Gakkhar, A dynamical model for HIV-typhoid co-infection with typhoid vaccine. *Journal of Applied Mathematics and Computing*, 1-30 (2021).

XI. Mousquer, G.T., A. Peres, M. Fiegenbaum, Pathology of TB/COVID-19 co-infection: the phantom menace. *Tuberculosis*, 126. 102020 (2021)

XII. Nicola, M., Z. Alsafi, C. Sohrabi, A. Kerwan, A. Al-Jabir, C. Iosifidis, M. Agha, R. Agha, The socio-economic implications of the coronavirus pandemic (COVID-19): A review. *International Journal of Surgery*, 78, 185-193 (2020)

XIII. Omame, A., U.K. Nwajeri, M. Abbas, C.P. Onyenegecha, A fractional order control model for diabetes and COVID-19 co-dynamics with Mittag-Leffler function. *Alexandria Engineering Journal*, 61, 7619-7635 (2022).

XIV. Omame, A., N. Sene, I. Nometa, C.I. Nwakanma, E.U. Nwafor, N.O. Iheonu, D. Okuonghae, Analysis of COVID-19 and comorbidity co-infection model with optimal control. *Optimal Control Applications and Methods*, 42(6), 1568-1590 (2021).

XV. World Health Organization, World Health Organization coronavirus disease (COVID-19) dashboard. *World Health Organization* (2020).

XVI. Polack, F.P., S.J. Thomas, N. Kitchin, J. Absalon, A. Gurtman, S. Lockhart, J.L. Perez, G. Pérez Marc, E.D. Moreira, C. Zerbini, Safety and efficacy of the BNT162b2 mRNA Covid-19 vaccine. *New England Journal of Medicine*, 383, 2603-2615 (2020).

XVII. Prieto Curiel, R., H. González Ramírez, Vaccination strategies against COVID-19 and the diffusion of anti-vaccination views. *Scientific Reports*, 11, 6626 (2021).

XVIII. Tang, B., X. Wang, Q. Li, N.L. Bragazzi, S. Tang, Y. Xiao, J. Wu, Estimation of the transmission risk of the 2019-nCoV and its implication for public health interventions. *Journal of Clinical Medicine*, 9, 462 (2020).

XIX. Tasman, H., An optimal treatment control of TB-HIV coinfection. *International Journal of Mathematics and Mathematical Sciences*, 2016, 1-10 (2016).

XX. Van den Driessche, P., J. Watmough, Reproduction numbers and sub-threshold endemic equilibria for compartmental models of disease transmission. *Mathematical Biosciences*, 180, 29-48 (2002).

XXI. Watson, O.J., G. Barnsley, J. Toor, A.B. Hogan, P. Winskill, A.C. Ghani, Global impact of the first year of COVID-19 vaccination: a mathematical modelling study. *The Lancet Infectious Diseases*, 22, 1293-1302 (2022).

XXII. Zhou, P., X.-L. Yang, X.-G. Wang, B. Hu, L. Zhang, W. Zhang, H.-R. Si, Y. Zhu, B. Li, C.-L. Huang, Addendum: A pneumonia outbreak associated with a new coronavirus of probable bat origin. *Nature*, 588, E6-E6 (2020).

XXIII. Hye, M.A., Biswas, M.H.A., Uddin, M.F., Rahman, M. M., A mathematical model for the transmission of co-infection with COVID-19 and kidney disease. *Sci Rep* 14, 5680 (2024).

XXIV. Hye, M.A., Biswas, M.H.A., Uddin, M.F,. Correction to: Mathematical Modeling of Covid-19 and Dengue Co-Infection Dynamics in Bangladesh: Optimal Control and Data-Driven Analysis. *Comput Math Model* 33, 388 (2022). 10.1007/s10598-023-09580-7